TECHNICAL TRANSACTIONS | CZASOPISMO TECHNICZNE
CIVIL ENGINEERING | BUDOWNICTWO
2-B/2015

SERGEY KUZNETSOV*, STANISLAV POSPÍŠIL*, RADOMIL KRÁL*

CLIMATIC WIND TUNNEL FOR WIND ENGINEERING TASKS

WYKORZYSTANIE TUNELU KLIMATYCZNEGO DO ZAGADNIEŃ INŻYNIERII WIATROWEJ

Abstract

This paper introduces a new climatic wind tunnel laboratory, which is one of the laboratories of the Institute of Theoretical and Applied Mechanics (ITAM) of the Academy of Science of the Czech Republic. The tunnel is used for fundamental research in civil engineering, architecture, and heritage care and in other fields where wind effects appear along with other factors. The paper includes essential information about the interior layout of the tunnel, descriptions of the principal parts of the tunnel which were designed taking into account both the optimal flow characteristics together with the description of some facilities serving for the simulation of a strong wind, rain, freeze and heat radiation, and the modelling of the atmospheric boundary layer. A design for a rectangular contraction nozzle, based on a parabolic profile and extending the capacity of the wind tunnel is presented.

Keywords: *climatic tunnel, wind tunnel, atmospheric boundary layer, flow resistance, wind tunnel contraction*

Streszczenie

Artykuł opisuje nowy tunel klimatyczny, który stanowi jedno z laboratoriów Instytutu Mechaniki Teoretycznej i Stosowanej (ITAM) Akademii Nauk Republiki Czeskiej. Tunel jest wykorzystywany do badań podstawowych z zakresu inżynierii lądowej, architektury i ochrony zabytków oraz w innych dziedzinach, w których pojawia się oddziaływanie wiatru wraz z innymi czynnikami zewnętrznymi. Artykuł zawiera kluczowe informacje o układzie wnętrza tunelu, opis jego głównych części, które zaprojektowano z uwzględnieniem optymalnej charakterystyki przepływu i z uwzględnieniem atmosferycznej warstwy przyściennej oraz opis urządzeń służących do symulacji silnego wiatru, deszczu, zamarzania i promieniowania ciepła jak . Zaprezentowano opis konstrukcji konfuzora, utworzonego w oparciu o profil paraboliczny, który zwiększa możliwości tunelu.

Słowa kluczowe: *tunel klimatyczny, tunel aerodynamiczny, atmosferyczna warstwa przyścienna, opór przepływu, konfuzor*

DOI: 10.4467/2353737XCT.15.139.4176

* Climatic Wind Engineering Laboratory CET, ITAM, Czech Republic.

1. Introduction

The Centre of Excellence Telč (CET) [13, 14] for research on materials and structures (particularly historic materials and structures) is equipped with a unique infrastructure designed and manufactured to enhance fundamental knowledge and to verify the application and innovation potential of newly developed technologies in the domain of diagnostics, life cycle extension, preventative protection and conservation. The CET consists of many laboratories, one of which is a climatic wind tunnel that has an environmentally and economically optimized size. The laboratory has both on-site developed and commercial measuring equipment for the industrial aerodynamics as well as for the flow visualization.

The scientific objective of climatic wind tunnel CET (CWT CET) is to create models of the interactions between solid bodies and the surrounding environment, utilizing the findings about wind load on structures, including monuments, and taking into account the influence of other weather factors, e.g. cyclic changes in temperature and exposure to rain. A further objective is to obtain new findings and knowledge by means of long-term sustainable monitoring and modelling of the behaviour of real structures exposed to long-term weather effects and susceptible to vibrations and to damage caused by high-cycle fatigue. Using appropriate models, the research leads to proposals for measures to provide a more comfortable environment in housing estates and in the neighbourhood of transport structures.

2. Description of CET wind tunnel

The wind tunnel is designed as a closed circuit with controlled wind velocity and temperature conditions. It consists of climatic and aerodynamic sections see Fig. 1. While the aerodynamic section provides well-fitted conditions to study wind effects on scaled models of prototypes, a piece of equipment of the climatic section is suited for investigations on the influences of weather including the wind, temperature, rain and heat radiation. Using the cooling/heating exchanger, cyclic temperature changing of the airflow is available in the whole tunnel within the range of –10 to +40°C in a relatively short time period. The integral part of the tunnel equipment consists of instruments for airflow diagnostics, data acquisition system, direct pressure surface measurements, precise thermometry and many other types of handy accessories for instant use. It is a unique wind laboratory at this size, while there is one such climatic laboratory in Europe, though much larger, residing in the CSTB research facility in Nantes, France see Barlow et al. [1].

The aerodynamic section consists of a converting nozzle with a honeycomb and the working part with a turning table. The working part is in a rectangular cross-section area of 1.9 × 1.8 m, the total length of the working part is 11.0 m. High quality airflow with low turbulence of about 1% is achieved in the free aerodynamic section without turbulence generators. The converting nozzle placed upwind compresses the incoming flow at ratio of 2.85. It increases wind speed at approximately the same rate and forms the airflow uniformity over the rectangular cross-section with the maximal wind speed exceeding 30 m/s.

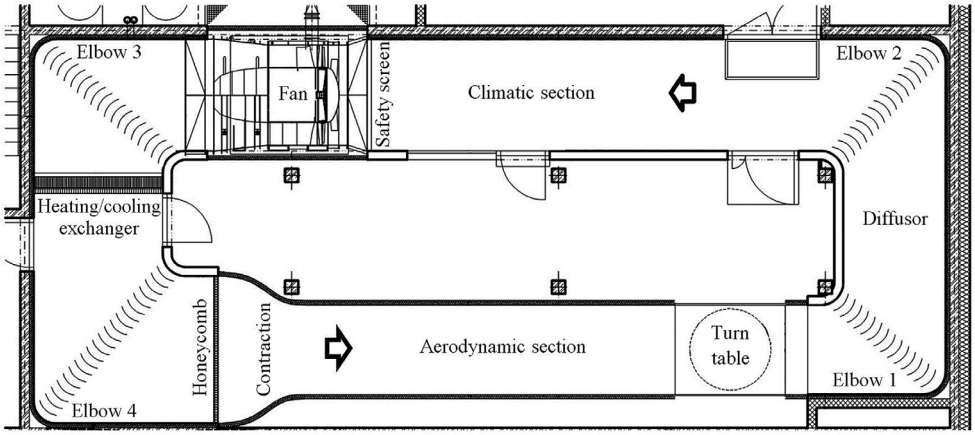

Fig. 1. Ground plan of the wind tunnel, designed in a near-oval closed shape adapted for aerodynamic and climatic testing, respectively. Arrows point in the wind direction

Using the diffusion passage and the pair of elbows, the cross-section expands twice towards the climatic chamber. To make the climatic section versatile for various types of experiments as much as possible, the ceilings with a sprinkler system and infrared lamps are continuously adjustable in height independently and over a wide range, see Fig. 2. The transition zone between the fixed tunnel roof and the sliding ceiling with the sprinklers is ensured with a rotationally adjustable flap. This chamber is in a rectangular cross-section of 2.5 × 3.9 m with a length of 9.0 m. The wind speed ranges are regulated by the position of the vertically moveable ceiling and flow nozzle from 0.8 to 30 m/s. The rain intensity together with the size of drops is regulated to simulate effects corresponding to drizzle or heavy rain. The radiation system with four infrared lamps with a total power of 8 kW, and maximal incidence of 60° to the floor, is available. The power is regulated to a large full extent and, if needed, just one lamp can be in operation.

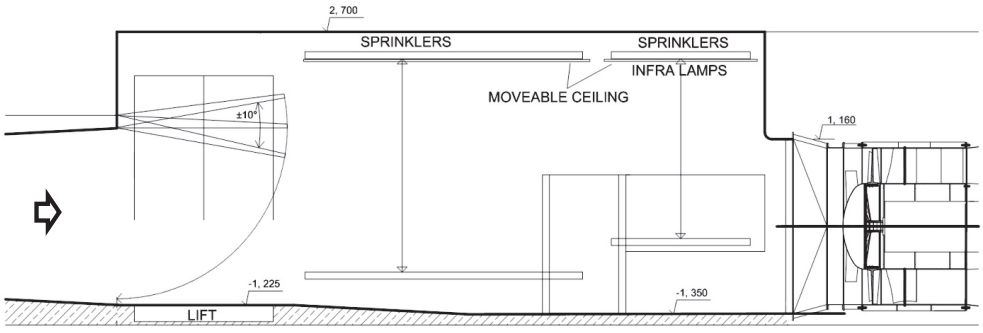

Fig. 2. Side view of the climatic section. The wind approaching from left can be adjusted by the nozzle and the moveable ceilings provide the flat plane towards the fan

Further downwind, the ventilator, an exchanger unit for air cooling/heating is integrated into the entire cross-section in a place with relatively low wind velocity (see Fig. 3). It consists of very thin aluminium ribs put next to each other on a distribution pipe with a small gap. The exchanger also functions as a screen considerably reducing the non-uniformity turbulence of flow generated by the ventilator. This arrangement shortens the disturbed zone behind the propeller by equalizing the wind speed distribution over the cross-section and prepares favourable airflow conditions for the aerodynamic section.

Fig. 3. Downwind view on aerodynamic section with historic tower model (left); View on the climatic chamber with 200 kW fan (right)

The airflow temperature is one of the main parameters of the climatic tunnel, it is measured and controlled from the control system of the wind tunnel. The design of the cooling capacity of the liquid-air heat exchanger takes into account three basic forms of heat gain: dissipative heat generated by air flow friction; accumulated heat in the tunnel structure and internal air; heat transfer due to the temperature gradient between the tunnel and surroundings. In order to minimize the energy consumption of the cooling unit, aluminium-wool or polystyrene insulation material was used on the outer walls.

The air humidity parameter is not controlled and its value is only monitored. In certain unfavourable cases at temperatures below zero, repeated condensing of the air moisture on the cooling exchanger can be used to decrease the humidity. This procedure serves for the reduction of ice accretion causing a potential decrease in the cooling efficiency and rise of pressure losses in the heat exchanger.

The wind tunnel is equipped with a sprinkler system. The rain intensity together with the size of drops is regulated to simulate effects corresponding to drizzle or heavy rain. Up to eighteen spray heads mounted on a moveable frame generate water drops using aerosol drifted with the air current towards the specimen. Afterwards, water is collected at several floor drains located at suitable places. The researchers can also use the infrared lamps for simulation of the temperature and solar radiation. The humidity generated with the sprinkler system brings increased demands on materials used both for the tunnel core itself and for the principal equipment. The material surface protection or non-corrosive materials have been used.

The majority of the tunnel devices are fully controlled by a central computer. This brings the possibility to schedule a test plan in advance using a common spreadsheet document and after importing, automatically execute the given tasks in chronological order. Because of remote access via internet and two cameras installed in both test sections, the tunnel can be controlled from a remote computer, tablet or smartphone with live video streaming.

3. Determination of the pressure losses

Two methods of determination were used. The first follows on from the experimental work by Fried and Idelchik [2] that provides a solution of fundamental cases appearing in internal fluid engineering problems. While the straight portions with a constant cross-sectional profile did not exhibit any significant issue, increased attention was paid to the tunnel components with complex shapes such as the contraction duct, elbows and screens. Starting from the basic arrangement as introduced in [2], step-by-step modelling consisting of slight changes in geometry was applied in order to achieved an optimal geometry from both the flow characteristic and flow resistance point of view. The numerical solution using direct Numerical Simulation in COMSOL was carried out to determine the pressure losses at the corners and to compare with empirical knowledge. In Fig. 4, velocity field distributed over the elbow area is presented. The picture on the left hand side shows the elbow behind the aerodynamic test section.

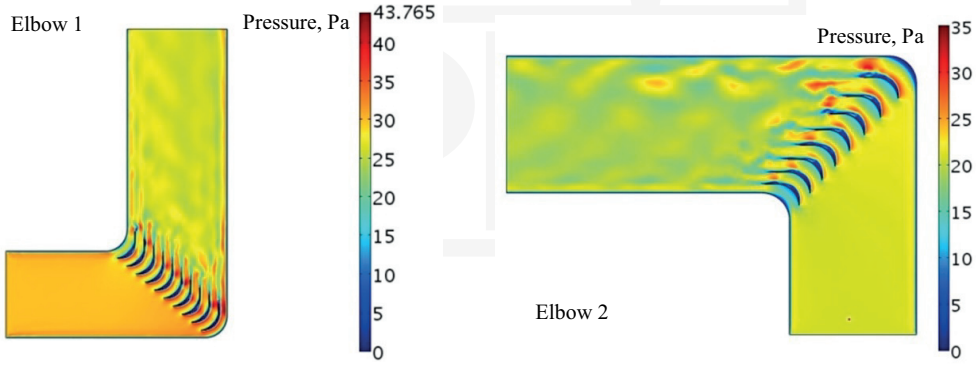

Fig. 4. Velocity field formed through the tunnel elbows: fine distribution of vanes is used for the elbow placed downwind from the aerodynamic section (left); for the remaining elbows, coarser spacing is employed (right)

Table 1 gives values of the pressure drop at certain points in the wind tunnel. Results according to Idelchik's guide are tabulated in the second column, while the last one expresses the contribution to overall pressure losses. Finally, values in the middle represent numerical results. Good results agreement was achieved although only a two-dimensional numerical model of CFD was employed. In Fig. 5, the results are processed in graphical form.

Table 1

Pressure losses of tunnel components by empirically and numerically determined values for maximal designed wind velocity

Flow passage	Empirical method [Pa]	Numerical method [Pa]	Total [%]
aerodynamic section	38		5
elbow 1	150	135	20
diffusor	3		0.4
elbow 2	70	57	
tube	1.8		0.25
climatic section	3.4		0.45
safety screen	37		4.9
fan	–	–	–
elbow 3	33	25	4.3
tube	0.6	–	0.1
heating/cooling exchanger	345	–	46
elbow 4	15	10	3.5
honeycomb	15	–	2
contraction duct	26	25	3.4

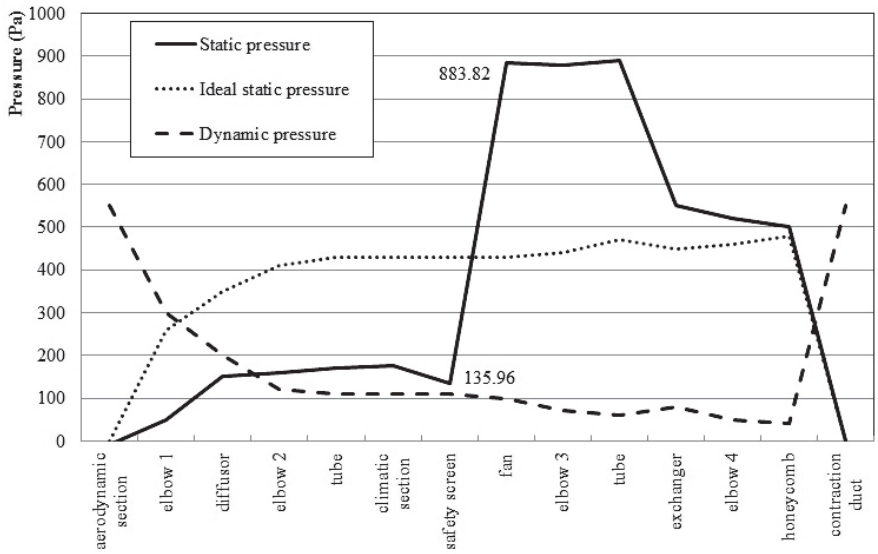

Fig. 5. Pressure development along the longitudinal centreline. The thick line represents an estimation of static pressure including flow resistance of tunnel elements

The dotted line represents the ideal static pressure determined regardless of the pressure losses. Provided that the losses are respected, a strong discontinuity appears being represented by the thick line. This jump clearly shows the required pressure gain of the fan to overcome the losses emerging when the maximal wind speed requirement is met. A 20% pressure reserve was used for the final design.

4. Atmospheric boundary layer modelling in CWT CET

The modelling of atmospheric boundary layers (ABL) is based upon well-established procedures as described by, among others, Cook [3] and Cermak [4]. The fundamental principles were originally suggested by Jensen [5]. Due to the long working part of the aerodynamic section of the tunnel, a satisfactory representation of the ABL can be obtained by the methods described below. The simulation of the ABL with demanded characteristics is based upon turbulent elements, such as spires, grids, and barrier and floor roughness (see Fig. 6). The influence of secondary recirculation in the working part is removed by means of barrier devices just after the contraction. Before these were installed, the flow near the floor at the downstream end of the test part was far from being horizontally homogeneous. Boundary-layer thickness can be increased without significant loss of similarity with the ABL by introduction of augmentation devices at the test-section entrance provided that the test-section is sufficiently long for the flow structure to reach statistical equilibrium.

Fig. 6. Atmospheric boundary layer modelling by vortex generator array, roughness elements and the barrier

An acceptable simulation of several category terrains for various scales (basically for 1:100) was obtained in the CWT CET.

The asymptotic matching of the similarity laws applicable to boundary layers which are governed by two characteristic length scales provides formal derivation of the 'logarithmic' velocity profile, while coupling the flow in the outer layer with the flow in the inner layer. A convenient empirical formulation often used for boundary layers in general is the 'power law' given by the following equation:

$$\frac{V(z)}{V(z_r)} = \left(\frac{z}{z_r}\right)^{1/\alpha} \tag{1}$$

where $V(z)$ is mean flow speed at height z, z_r is a reference height, $1/\alpha$ is exponent in power law approximation boundary layer. Vertical profiles for the four terrain categories according to Eurocode [6] and the testing campaign using vortex generators, spires and roughness elements (full ABL for the terrain category IV) are presented on the Figure 7. Spires in

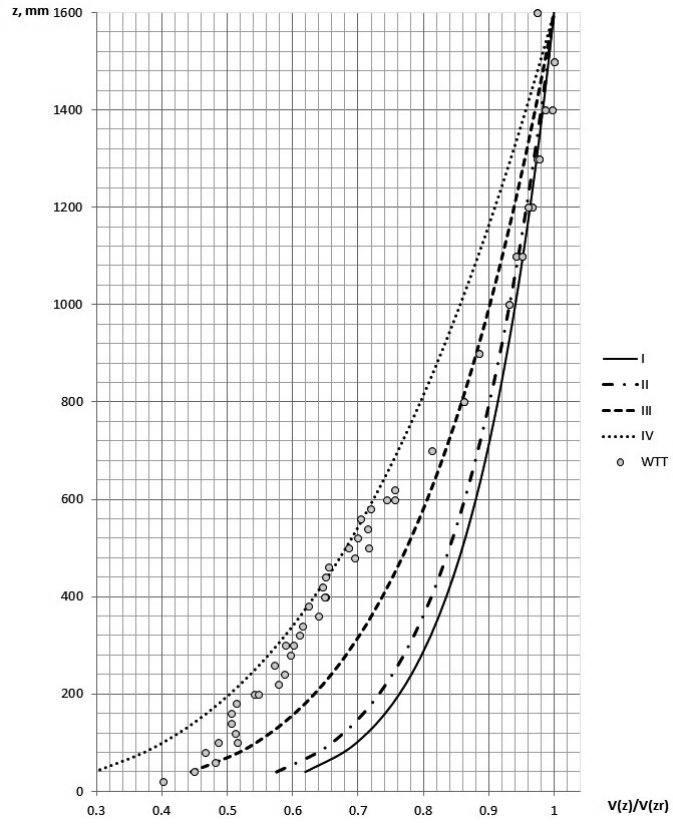

Fig. 7. Vertical profiles of mean velocity in the wind tunnel tests (WTT) compared with empirical calculation for terrain categories according to Eurocode [6] (I is rough, open sea, lakes and smooth flat country without obstacles; II is farmland with boundary hedges, occasional small farm structures, houses or trees; III is suburban or industrial areas and permanent forests; IV is urban areas in which at least 15% of the surface is covered by buildings with an average height exceeding 15 m)

the flow-processing section were combined with a block evenly distributed in the working section. The turbulent length scale of the boundary-layer flow was thereby much improved. Urban boundary layers formed over rough surfaces and approached equilibrium more rapidly through enhanced diffusion than those formed over relatively smooth surfaces.

Turbulent flow velocities vary randomly in both time and space and can be expressed either in terms of their spectral characteristics or in brief, by auto or cross-power spectral densities S_{ivv}. Statistics of primary interest for wind engineering applications are variances and standard deviations σ_i, the integral length scales ${}^{j}L_i$ for the *i*-th velocity component and *j*-th coordinate direction. Knowing the dispersion, turbulence intensity is given by the following formula:

$$I_u(z) = \frac{\sigma_j(z)}{V(z)} \tag{2}$$

The measured turbulence intensity profiles are presented in Figure 8. In the lower part of the ABL, near to the ground, is an intensity of around 27% when using the equipment as shown in Fig. 6.

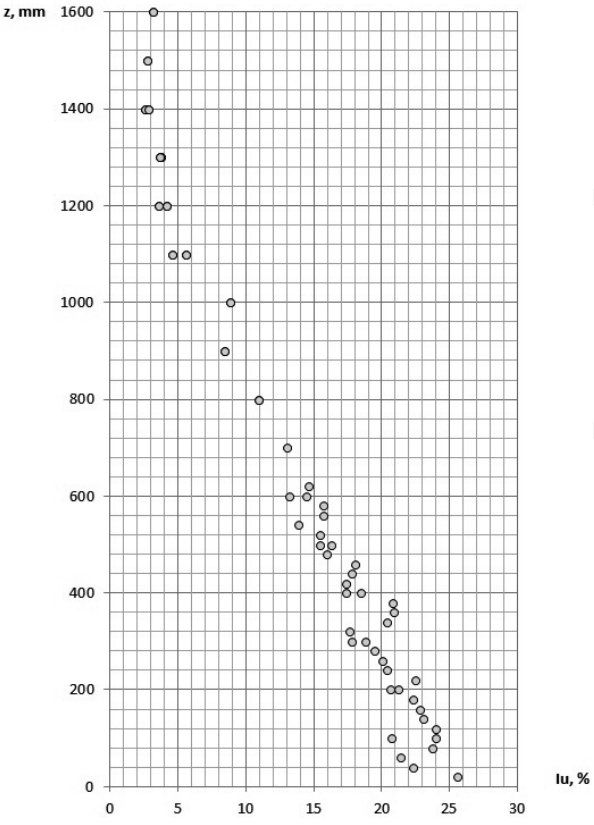

Fig. 8. Vertical profile of longitudinal turbulence intensity obtained from the wind tunnel tests

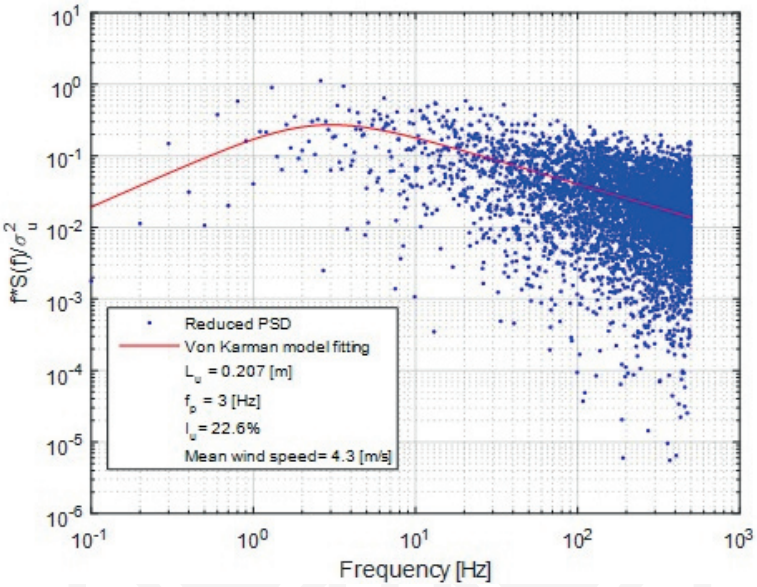

Fig. 9. Longitudinal turbulence spectra in the wind tunnel. Best fitting curve is given by the von Karman spectrum

Figure 9 shows an example of wind speed power spectral density for some point in the lower part of the ABL. Low-frequency side of a velocity spectrum corresponds to the large scale turbulence (which corresponds to large eddies in the flow and hence defines the integral length scale). The high frequency part of the spectrum, however, corresponds to small eddies in the flow (small-scale turbulence).

5. Inbuilt high speed nozzle

An important characteristic of a wind tunnel is the flow quality inside the test chamber and the overall performance. The three main criteria that are commonly used to define them are: maximum achievable speed; flow uniformity; turbulence level-intensity. Therefore, in general, the aim of contraction design is to get a better controlled flow in the test chamber, achieving the necessary flow performance and quality parameters.

Besides the stationary elements for the atmospheric flow simulation, the authors have designed a rectangular contraction nozzle, based on a parabolic profile for the significant enhancement of the aerodynamic measurements in a climatically wind tunnel – this provides a better controlled flow in the test chamber, achieving the necessary flow performance and quality parameters [7, 8]. To describe and characterize its performance, intensive experimental measurements have been conducted using pressure transducers and hot-wire anemometry.

The design of a contraction of a given area ratio and cross-section centres on the production of a uniform and steady stream at its outlet and requires the avoidance of flow separation within it. Another desirable flow quality is a minimum boundary layer thickness (in a laminar state) at the contraction exit [9–12]. This suggests that the contraction length should be minimized in order to minimize the boundary layer growth. Shorter contractions are also, of course, desirable for saving in the aerodynamic section space. However, the risk of boundary layer separation increases as the contraction length is reduced.

A long contraction produces better results for the fulfilment of these requirements. However, very long contraction leads to an increase of the boundary layer along walls and also the aerodynamic section of CET climatic wind tunnel cannot be fully used for this. The length of the contraction should be thus in the range from 1.5 to 2.5 of the outlet diameters (according to our experiences). Cylindrical section is located between the contraction and the working part to ensure a smooth transition and radius of cylinders should be 0.1–0.2 outlet diameter of the contraction.

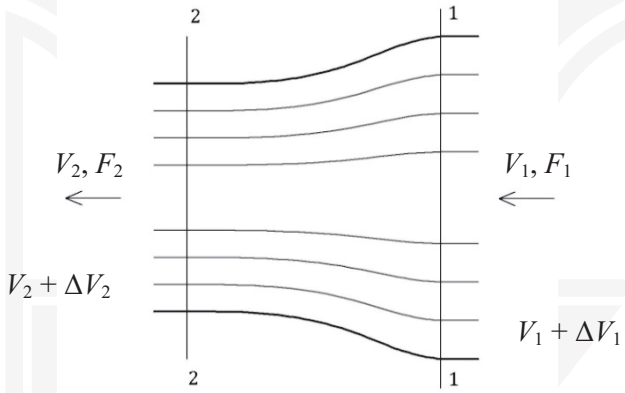

Fig. 10. Flow streamlines of the contraction

The aligning action of the contraction can be determined from the following description: in the cross-section F_1 No. 1 (inlet of the contraction, see Fig. 10); one of a streamline has velocity is V_1 and another is $V_1 + \Delta V_1$ wherein a cross-section pressure is constant, similarly for the cross-section F_2 No. 2 where V_2 and $V_2 + \Delta V_2$ (outlet of the contraction, see Fig. 10). Bernoulli equation has been formulations for both sides and obtained the following:

$$V_1 \Delta V_1 = V_2 \Delta V_2 \quad \text{or} \quad \Delta V_1 = \Delta V_2 \frac{V_2}{V_1} \tag{3}$$

The uniformity of flow velocity can be used as follows:

$$a_1 = \frac{\Delta V_1}{V_1} \quad \text{and} \quad a_2 = \frac{\Delta V_2}{V_2} \tag{4}$$

$$a_1 = \Delta V_2 \frac{V_2}{V_1^2} = \Delta V_2 \frac{V_2}{\left(\frac{V_2}{n}\right)^2} = n^2 a_2 \tag{5}$$

where n is contraction ratio and $n = V_2/V_1 = F_1/F_2$. Thus, the uniformity of outlet flow velocity n^2 times less than the uniformity of inlet flow velocity of a contraction. After some optimization steps, the shape of the contraction was determined according to the formula:

$$y = \frac{r_2}{\sqrt{1-\left[1-\left(\frac{r_2}{r_1}\right)^2\right]\frac{\left(1-3x^2/\left(4r_2\right)^2\right)^2}{\left(1+3x^2/\left(4r_2\right)^2\right)^3}}} \tag{6}$$

where x is along stream direction coordinate, r_1 is radius of inlet cross-section, r_2 is radius of outlet cross-section.

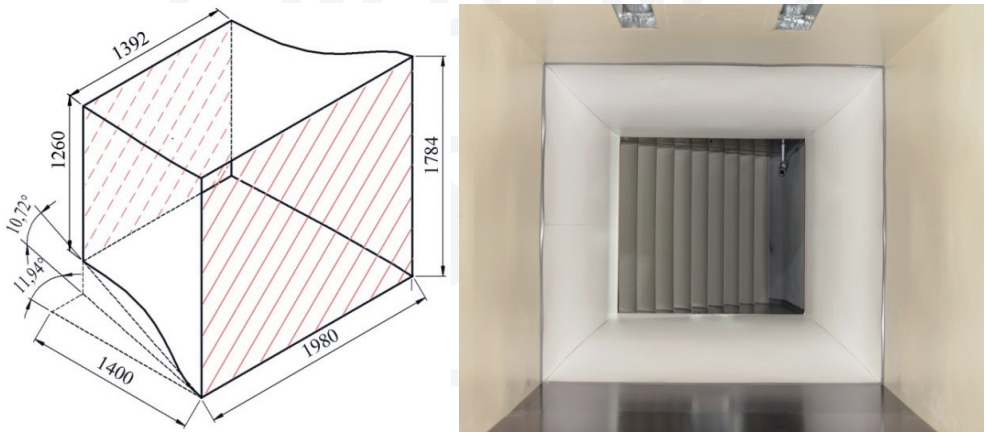

Fig. 11. The high speed chamber: geometrical parameters of the contraction (left), the downstream view (right)

The contraction resulted in the increase of speed up to 55 m/s. Turbulence intensities below 0.3% were obtained for the whole range of velocities. Constant uniform flow was obtained for all the cross-sections along the nozzle. These indicators show that the special contraction nozzle is an excellent enhancement improving wind tunnel performance.

The quality of the flow has changed due to the compression of air stream and reducing of the contraction outlet cross-section area. The uniformity velocity distribution was 0.7 % in accordance with the experimental results (see Fig. 12).

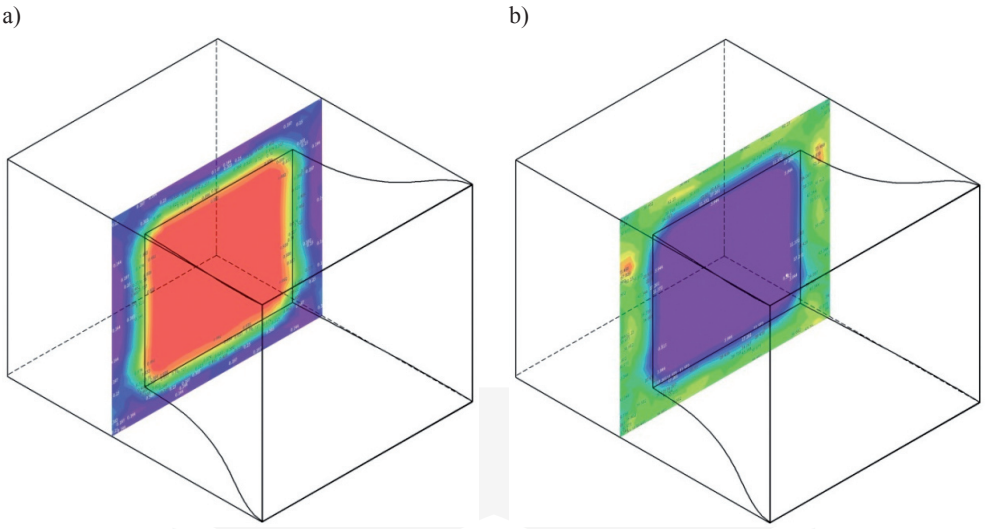

Fig. 12. Flow characteristics of the working section: a) velocity; b) turbulence

6. Conclusions

This paper presents a description of the newly-built wind tunnel developed for fundamental research of engineering problems related to the study of wind and climatic effects on structures. The paper describes the pressure loss determination and other important design issues. The unique wind climatic tunnel uses a combination of two working sections. This arrangement is advantageous due to its wide universality and adaptability to experimental demands. Besides the interior layout tunnel description, the full paper focuses on the description of the flow resistance of essential tunnel parts, the modelling of atmospheric boundary layers and the design of a rectangular contraction nozzle.

This work was supported by the European Regional Development Fund of the project CZ.1.05/1.1.00/02.0060, the project GAČR 14-12892S, the Ministry of Education, Youth and Sports, and the Academy Sciences of the Czech Republic

References

[1] Barlow J., Rae W.H., Pope A., *Low-speed wind tunnel testing*, John Wiley & Sons, USA, 1999.

[2] Fried E., Idelchik I.E., *Flow resistance: A design guide for engineers*, Taylor & Francis, London 1998.

[3] Cook N.J., *The designer's guide to wind loading of building structures*, Part 1, Butterworths, London 1985.

[4] Cermak J.E., *Development of wind tunnels for physical modeling of the atmospheric boundary layer*, [In:] *A State of the Art in Wind Engineering*, Davenport Sixtieth Birth Anniversary Volume, Wiley Eastern Limited, USA, 1995, 1-25.

[5] Jensen M., *The model law for phenomena on natural wind*, Ingeniøren, Int'l Edition, 2, 1958, 121-128.

[6] Eurocode 1: Actions on structures − Part 1–4: General actions − Wind actions.

[7] Fang F., *A design method for contractions with square end sections*, Journal of Fluids Engineering, Vol. 119, 1997, 454-458.

[8] Mehta R., *The aerodynamic design of blower tunnels with wide-angle diffusers*, Progress in Aerospace Sciences, Vol. 18, 1979, 59-120.

[9] Fang F., Chen J., Hong Y., *Experimental and analytical evaluation of flow in a square-to-square wind tunnel contraction*, Journal of Wind Engineering and Industrial Aerodynamics, Vol. 89, 2001, 247-262.

[10] Song C.C.S., Yuan M., *A weakly compressible flow model and rapid convergence methods*, Journal of Fluids Engineering, Vol. 110, 1988, 441-455.

[11] Wolf T., *Design of a variable contraction for a full-scale automotive wind tunnel*, Journal of Wind Engineering and Industrial Aerodynamics, Vol. 56, 1995, 1-21.

[12] Michalcová V., Kuznetsov S., Brožovský J., Pospíšil S., *Numerical and experimental investigations of air flow turbulence characteristics in the wind tunnel contraction*, Applied Mechanics and Materials, Vol. 617, 2014, 275-279.

[13] http://www.itam.cas.cz

[14] http://cet.arcchip.cz